PHOTO-DEGRADATION OF METHYLENE BLUE USING CLAY SUPPORTED V_2O_5-TiO_2 NANO-COMPOSITES

A

Thesis submitted

In partial fulfilment of the requirements for the degree of

MASTERS OF SCIENCE

IN

CHEMISTRY

Submitted by

SHRUTI PARASHAR

(301502033)

Under the Supervision of

Dr. SOUMEN BASU

(Associate Professor)

SCHOOL OF CHEMISTRY & BIOCHEMISTRY

THAPAR UNIVERSITY, PATIALA

July, 2017

CERTIFICATE

I hereby declare that the thesis entitled **"Photo-degradation of methylene blue using clay supported V_2O_5-TiO_2 nano-composites"** is an authentic record of my work carried out as requirements for the award of the degree of Master of Science in Chemistry at Thapar University, Patiala under the supervision of Dr. Soumen Basu, Associate Professor, School of Chemistry & Biochemistry, Thapar University, Patiala during July' 2015 to July' 2017. No part of the matter embodied in this report has been submitted to any other university or institute for the award of any degree.

Date: 17th July, 2017

Shruti Parashar

It is certified that the above statement made by the student is correct to the best of my knowledge and belief.

Dr. Soumen Basu
Associate Professor
School of Chemistry & Biochemistry
Thapar University, Patiala - 147004

CANDIDATE'S DECLARATION

I hereby declare that the work being presented in the dissertation entitled **"Photo-degradation of methylene blue using clay supported V_2O_5-TiO_2 nano-composites"** in partial fulfilment of the requirements for the award of degree of Masters of Science in Chemistry and being submitted to School of Chemistry and Biochemistry, Thapar University, Patiala, is my own work during the period of January' 2017 to July' 2017, under the supervision of **Dr. Soumen Basu.** I have not submitted the contents embodied in this dissertation for the award of any other degree.

Patiala
Date: 17th July 2017

Shruti Parashar

This is to certify that the statement made by the candidate is correct and true to the best of our knowledge.

Dr. Soumen Basu
Associate Professor
School of Chemistry & Biochemistry
Thapar University, Patiala – 147004

ACKNOWLEDGEMENT

First of all, I owe my gratitude to the Head of the Department, **Dr. Amjad Ali** for providing me an opportunity in the form of this dissertation to develop my interest in research.

In the same spirit, I would like to thank my Supervisor, **Dr. Soumen Basu** for his constructive guidance and constant support during the project. The work presented here could not have been accomplished without his patience and ever willingness to teach. He has taught me to be concise and correct in my approach from the formulation of ideas to the presentation of the results.

Special thanks to all the **Teaching Faculty** of the department for their cooperation and guidance.

I would also like to express my gratitude to **Ms. Akansha Mehta**, **Mr. Amit Mishra**, **Ms. Shagun Kainth**, **Ms. Manisha Sharma**, **Ms. Dimple Garg** and **Ms. Nidhi Arora** who never turned me down whenever I approached them for any kind of help. Also, thanks to all the research scholars for their assistance.

I am grateful to **School of Chemistry & Biochemistry, Thapar University** for providing financial support and all necessary infrastructure and laboratory facilities to carry out the experimental work.

Words fail me to express my thanks to my family and friends who have always supported me and have been a source of strength and inspiration to me during the entire period of the work.

All these thanks are, however, only fraction of what is due to almighty for granting me an opportunity and strength to successfully accomplish this project.

ABSTRACT

Clay supported TiO_2-V_2O_5 nano-composites were synthesised using microwave technique. Three different samples were prepared by varying the composition of V_2O_5 with respect to clay-TiO_2. The synthesized nano-composite was analysed using X-ray diffraction, diffuse reflectance spectroscopy, Brunauer - Emmett - Teller and Transfer Electron Microscopy. Their photocatalytic activity was compared to that of clay-TiO_2 and commercially available p25 by degrading methylene blue with a catalytic dose of 0.25g per litre in 20 ml (10^{-4} M concentration) of dye. The degradation was carried out in both UV and visible light. It was found that presence of V_2O_5 along with clay-TiO_2 effectively enhanced the catalytic activity of clay-TiO_2 and caused dye to degrade totally in both UV and visible light.

Keywords:

Clay, methylene blue, photocatalytic, degrade, TiO_2, V_2O_5.

CONTENTS

LIST OF FIGURES

LIST OF TABLES

LIST OF ABBREVIATIONS AND SYMBOLS

1.	**MB**	Methylene blue
2.	**%**	Percent
3.	**<**	Less than
4.	**>**	Greater than
5.	**µm**	Micrometre
6.	**a.u.**	Arbitrary unit
7.	**AOP**	Advanced oxidation processes
8.	**BET**	Brunauer-Emmett-Teller
9.	**CFL**	Compact Fluorescent Light
10.	**CTAB**	Cetyl trimethyl ammonium bromide
11.	**DRS**	Diffuse reflectance spectroscopy
12.	$\mathbf{e^-}$	Electrons
13.	$\mathbf{E_{bg}}$	Band gap energy
14.	**EM**	Electromagnetic
15.	**eV**	Electron volts
16.	**gm**	Gram
17.	**h**	Planck's constant
18.	$\mathbf{h^+}$	Holes
19.	**HTAB**	Hexadecyl trimethyl ammonium bromide
20.	**IR**	Infrared
21.	**kV**	Kilovolt
22.	**L**	Litre
23.	**m**	Metre
24.	**MALDI**	Matrix-assisted laser desorption ionization
25.	**mg**	Milligram
26.	**Min**	Minute
27.	**mL**	Millilitre
28.	**MMT**	Montmorillonite

29.	**Mol**	Mole
30.	**MW**	Molecular Weight
31.	**nm**	Nanometre
32.	**NPs**	Nanoparticles
33.	**^{o}C**	Degree Celsius
34.	**Py**	Pyridine
35.	**θ**	Theta
36.	**RhB**	Rhodamine B
37.	**rpm**	Revolutions per minute
38.	**SDS**	Sodium dodecyl sulphate
39.	**SEM**	Scanning electron microscope
40.	**SEM**	Scanning electron microscope
41.	**TEM**	Transmission electron microscope
42.	**TEM**	Transmission electron microscopy
43.	**UV**	Ultra-violet
44.	***ν***	Frequency
45.	**W**	Watt
46.	**XPS**	X-ray photoelectron spectroscopy
47.	**XRD**	X-ray diffraction
48.	**ε**	Molar absorption coefficient
49.	**λ**	Wavelength
50.	**λ_{max}**	Maximum wavelength

CHAPTER-1

INTRODUCTION

1.1 Nano-composites

1.1.1 Definition

A *nanocomposite* means nano-sized particles (i.e. metals, semiconductors, dielectric materials, etc.) embedded in different matrix materials (ceramics, glass, polymers, etc). In simple terms, it is a matrix to which nanoparticles have been added to improve a particular property of the material. It is a solid material which is multiphase. One of the phases has one, two or three dimensions of less than 100 nanometers (nm), or structures having nano-scale (10^{-9} m) repeat distances between the different phases that make up the material. They consist of two phases (i.e. nano-crystalline phase + matrix phase). Phase may be inorganic-inorganic, inorganic-organic or organic-organic. They are different from bulk material and isolated molecules because of their unique physical and chemical properties accounted to them having greater surface area per weight than larger particles causes them to be comparatively more reactive than some other molecules.

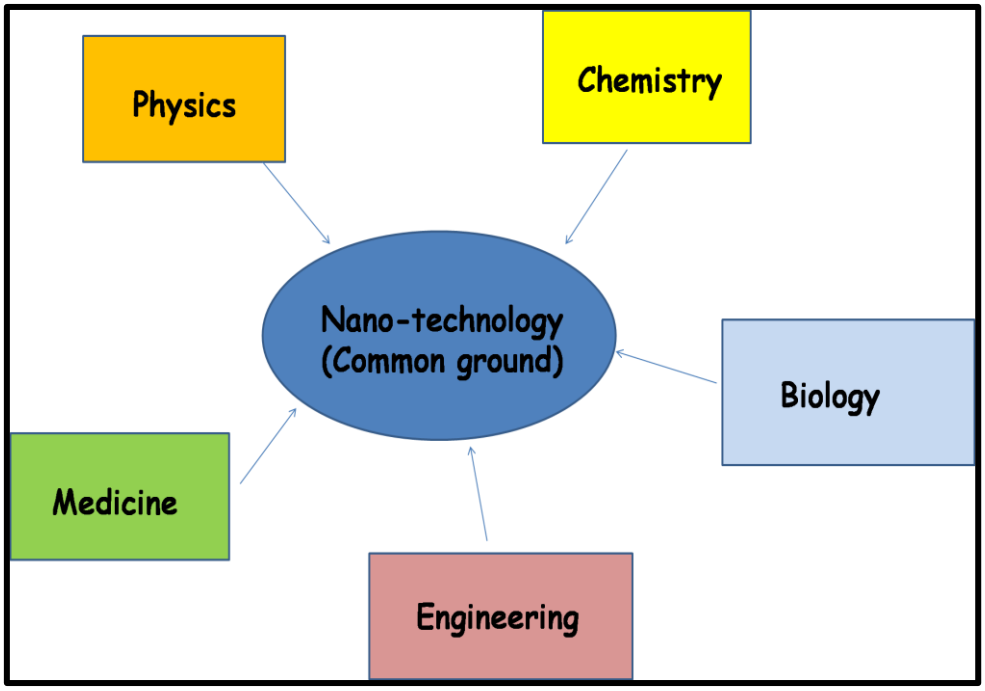

Fig. 1.1 Nano-technology as a common ground

1.1.2 Synthesis of nano-composites

They can be synthesized by various techniques including chemical reduction, sol-gel process, aero-gel process, hydrothermal routes, encapsulation in holes, co-precipitation and microwave synthesis. In the current research microwave technique has been used to synthesize clay-TiO_2 and clay TiO_2-V_2O_5 nano-composites.

1.1.3 Challenges faced in nano-technology

For the fabrication and processing of nano-particles there are various challenges that must be met. The challenges include overcoming the huge surface energy arising due to large surface area of nano-particles; ensuring that all nano-particles have desired size, uniform size distribution, morphology, chemical composition, crystallinity and microstructure that altogether results in desired physical properties; preventing nanomaterials and nanostructures from concerning through Ostwald ripening or agglomeration; and morphology control.

1.1.4 Applications of nano-composites

Nanocomposites can dramatically improve properties like:

- (Mechanical properties) Strength, modulus and dimensional stability
- Electrical conductivity
- Decreased permeability for water and gas hydrocarbons
- Flame retardancy
- Thermal stability
- Chemical resistance
- Surface appearance
- Optical clarity

Nanocomposites have an extremely high surface to volume ratio which dramatically changes its properties as compared to its bulk sized equivalents. Also, it changes the way in which the nanocomposites bind with the bulk material as a result of which the composite can be

improved many times with respect to the component parts. Some nanocomposite materials have been shown to be thousand times tougher than the bulk component materials.

Nanocomposites are currently being used in a number of fields and new applications are continuously being developed. Mentioned below are some of the applications of nanocomposites :

- Thin-film capacitors for computer chips
- Solid polymer electrolytes for batteries.
- Automotive engine parts and fuel tanks
- Impellers and blades
- Oxygen and gas barriers
- Food packaging

In the current research nano-composites of Clay supported TiO_2-V_2O_5 has been utilized for enhanced photocatalytic activity for degradation of methylene blue. [26]

1.2 Dye degradation

1.2.1 Dye degradation: Overview

It is defined as a process that degrades large dye molecules into smaller ones. Dye degrades to give water, carbon dioxide and mineral byproducts that provide colour to the original dye. After being released in the environment, dye molecules persist in the environment because most of them are unreactive towards oxygen, light, acids and bases [1].

1.2.2 Need for dye degradation

Industrial effluents such as dyes are one of the major causes of environmental pollution since discharge of dye containing wastewater from various industries such as textiles, printing, food and cosmetics poses a major threat to human and ecology since they are highly toxic and carcinogenic with a large amount of non-biodegradable suspended organic solid. Their presence even at low concentrations in water bodies not only degrades water quality but also obstruct the penetration of sunlight affecting the aquatic plant and animal life **[2, 3]**.

1.2.3 Methylene Blue (MB)

Methylene blue is a dye and medication. Medically, it is mostly used to treat methemoglobinemia. Earlier it was also used to treat Urinary tract infection (UTI) and Cyanide poisoning, but that use is no longer recommended. As a dye, it is a thiazine dye and because it is a cationic dye, therefore, its adsorption is favoured on a negatively charged surface at high pHs [4].

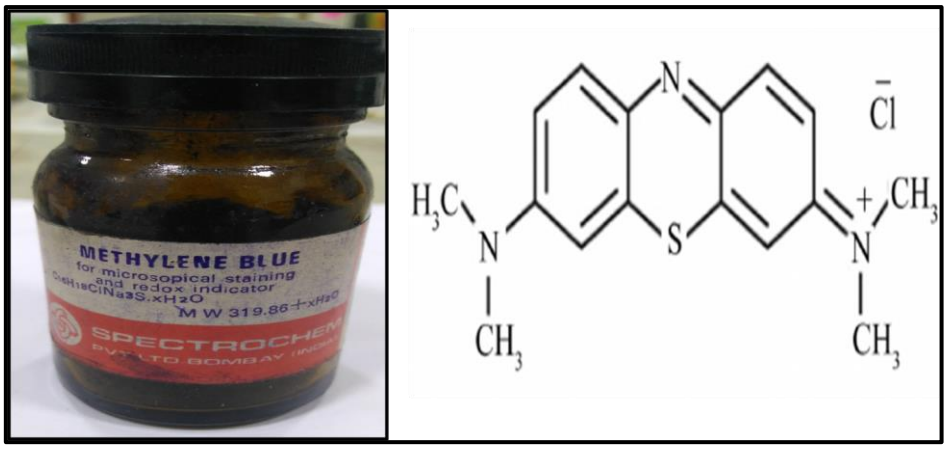

Fig. 1.2 Methylene Blue and its Structure.

1.2.4 Methods used for dye degradation

Physical methods such as adsorption, biological methods such as biodegradation and chemical methods such as chlorination, ozonation are the most frequently used for dye degradation [5].

Physical methods - Adsorption

Adsorption is defined as the adhesion of molecules, atoms, or ions from a gas, liquid, or dissolved solid to a surface. The process of adsorption creates a film of the adsorbate on the surface of the adsorbent. It is a surface phenomenon. It is vastly used in treatment procedures of dyes. Adsorbents (surface that adsorbs) are mainly derived from sources such as zeolites, clays, ores, charcoal, etc.

Biological methods - Biodegradation

Biodegradation is defined as the decomposition of materials by fungi, bacteria, or other biological means. Organic material can be degraded both aerobically (i.e. with oxygen) or anaerobically (i.e. without oxygen). Disintegraion of biodegradable substances can include both abiotic and biological steps.

Chemical methods

It is a chemical method used for disinfection that takes into use various types of chlorine or chlorine-containing substances for the oxidation and disinfection of water source.

These techniques transfer non biodegradable matter into sludge, thus they are non destructive. Advanced oxidation processes (AOP) or heterogeneous photocatalysis that leads to the complete decomposition of organic pollutants into H_2O and CO_2 [5, 6] is a new emerging technology.

1.3 Photocatalytic degradation

Defined as a process where, initially absorption of photons by a semiconductor takes place forming holes and electrons. The semiconductor band diagram has been explained in Fig. 1.3.

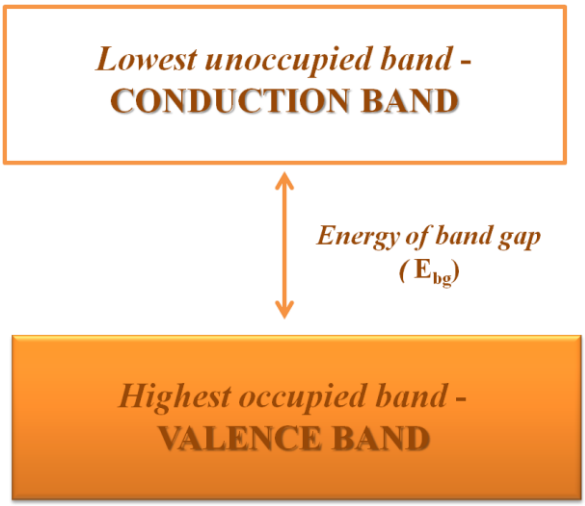

Fig. 1.3 Semiconductor band gap diagram

Now, E_{bg} has its values in the range of UV-Visible region (200 nm - 800 nm). Therefore, activation of the surface of semi-conductor with UV/Vis light leads to the excitation of electrons from the highest occupied band to the lowest unoccupied band, which in turn leads to generation of electron (e-) / hole (h+) pairs.

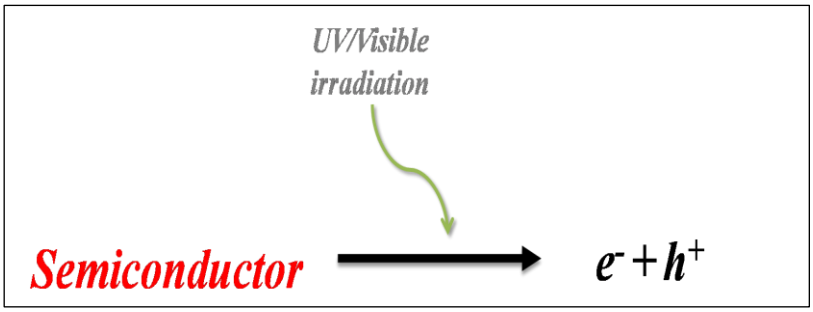

The initiation of a number of oxidation – reduction reactions takes place due to the e- /h+ pairs which get generated due to the photons. The mechanisms that are involved in these reactions have been discussed below:

1) Oxidation of adsorbed water molecules and hydroxyl ions by holes produced due to photons to give hydroxyl radicals

$$\text{hole} + OH^- \longrightarrow O\dot{H}$$

$$\text{hole} + H_2O \longrightarrow O\dot{H} + H^+$$

2) Reduction of dissolved oxygen via the e^- produced from photons to produce super oxide anions radicals, which results in the production of H_2O_2 through a series of redox reactions

$$O_2 + e^- \longrightarrow O_2^-$$

$$O_2^- + H^+ \longrightarrow HO_2^{\cdot}$$

$$HO_2^{\cdot} + HO_2^{\cdot} \longrightarrow H_2O_2 + O_2$$

$$O_2^- + HO_2^{\cdot} \longrightarrow HO_2^{-} + O_2$$

$$HO_2^- + H^+ \longrightarrow H_2O_2$$

The photo-generated H_2O_2 undergoes further decomposition to give OH radicals:

$$H_2O_2 + O_2^- \longrightarrow >O\dot{H} + O\dot{H}^- + O_2$$

$$H_2O_2 + e^- \longrightarrow >O\dot{H} + OH^-$$

3) Direct participation of holes in redox reaction.

$$H_2O_2 + h\nu \longrightarrow O\dot{H} + O\dot{H}$$

$$O\dot{H} + \text{dye} \longrightarrow \text{dye intermediate}$$

$$O\dot{H} + \text{dye intermediate} \longrightarrow CO_2 + H_2O + \text{end products}$$

4) A singlet oxygen may form which can take part in oxidation-reaction.

The primary oxidizing agents, i.e., O$\dot{H}$ radical, superoxide anion radical, and H_2O_2 are non-selective radicals that are strong and have the capability to initiate the oxidation reactions of adsorbed organic molecules. This oxidative reaction proceeds through numerous free radical reactions, wherein a variety of intermediates is produced. Furthermore, these undergo oxidative cleavage, which finally results in the formation of CO_2, H_2O and inorganic ions.

1.4 Photo-catalyst

A variety of photo-catalysts (generally sulphides of some metals or semiconductor oxide) that excite the electron/hole pairs to the state with higher energy are being utilized for degradation of dyes and organic pollutants. Among these photo-catalysts TiO_2 is the most widely used as

a photo-catalyst because it is cost effective, abundant, highly chemically stable, and less toxic.

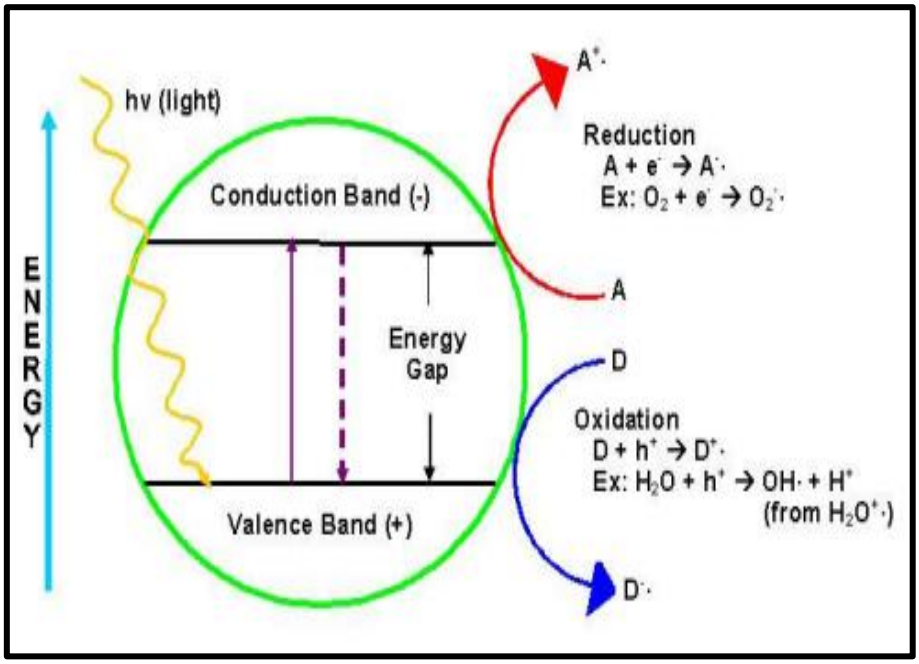

Fig. 1.4 Irradiation of TiO_2 particles

However, it has some major defects which hamper its large scale application as a photo-catalyst for water treatment. Firstly, it has low adsorption capacity, low surface area, non-uniform pore distribution and formation of uniform suspension in water which makes its recovery difficult. Also, it has a relatively high energy band gap ($Eg \approx 3.2$ eV), due to which it shows its activity only under ultraviolet (UV) region of sunlight ($\lambda < 400$ nm) [7], which constitutes only 10% of the total light output of the sun. This partially rules out its use in visible light.

Various efforts have been undertaken to overcome above mentioned limitations of TiO_2. In order to enhance its adsorption capacity, surface area and porosity, TiO_2 can be incorporated upon certain materials which can act as supports such as mesoporous silica, activated carbon, zeolites, clays etc. Among these clays have gained significant attention due to their layered structure, chemical and mechanical stability, cation exchange capacity, low cost, nontoxic nature and availability [8].

Clay-TiO_2 nanocomposites tend to possess high surface area, porosity and also large number of surface active sites [9]. Therefore, clay-TiO_2 nanocomposites have become one of highly promising materials for photocatalytic air and water purification. Based upon textural differences clays are primarily classified of two types which are 2:1 clay or MMT clays and 1:1 clay such as kaolin. Montmorillonite clays comprise of two tetrahedral silica layers and one octahedral alumina layer in between silica layers thus forming a category of 2:1 clays. The net negative charge generated due to lattice imperfection and isomorphic substitution enables absorption of alkaline and alkaline earth metal cations in interlayer space [10, 11]. Clay-TiO_2 nanocomposites have been synthesized by several reported methods such as Solvothermal [12], hydrothermal [13], microwave assisted method [14, 15] etc.

Moreover, in order to make TiO_2 active in visible region, it can be doped with V_2O_5. Vanadium having partially filled d-orbitals accounting for a wide variety of electronic, magnetic, and catalytic properties. Vanadium atoms can exist in multiple stable oxidation states results in the easy conversion between oxides of different stoichiometry by oxidation or reduction and is believed to be an important factor for the oxide to function as a catalyst in selective oxidation [16].

1.5 Characterization techniques

1.5.1 X-ray diffraction analysis

X-ray diffraction (XRD) is a non-destructive, powerful technique for characterizing crystalline materials**.** It provides information on phase, crystal structure, preferred crystal orientation (texture), and other structural parameters that are crystallinity, average grain size, crystal defects and strain. It is based on constructive interference of monochromatic X-rays and a crystalline sample: The X-rays are generated by a cathode ray tube which are further filtered to produce monochromatic radiation, collimated to concentrate, and then directed toward the sample. In this dissertation the crystallinity and phase of the synthesises nano-composites was determined from XRD using PANALYTICAL X-ray diffractometer operating at 45kV having Cu Kα (λ = 0.154 nm) as X-ray source. Sample scan range was kept from 20° to 80°.

Fig. 1.5 XRD instrument

1.5.2 Nitrogen Sorption Analysis

One of the characteristic properties of a nano-composites is its pore structure. Nitrogen adsorption-desorption isotherms data were used in the experiments conducted as part of this dissertation to obtain information about specific surface area and pore structure parameters of the synthesized materials. In the present work, surface area and porosity were analyzed using MICRO TRACBEL surface area analyzer (Fig. 1.7). Before analysis, 100mg sample was pre-treated at 150℃ for 3 hours.

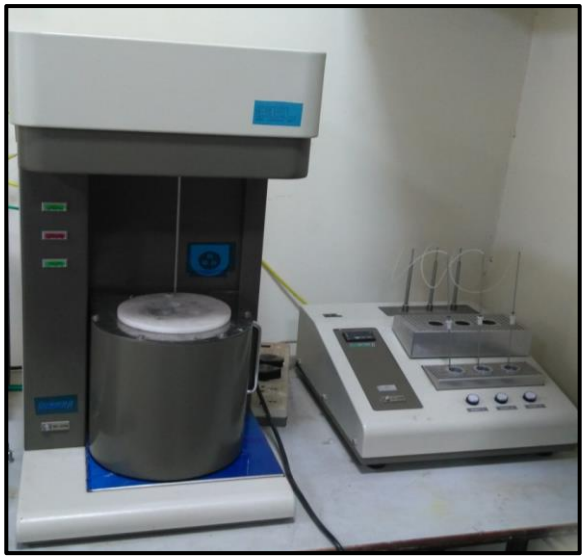

Fig. 1.6 MICRO TRACBEL surface area analyzer

As shown in Figure 1.8, gas adsorption isotherms have been classified by IUPAC into six different types. Type I is a characteristic adsorption isotherm from microporous solids. Types II, III, and VI are obtained due to adsorption in non-porous or macroporous materials, and Types IV and V arise from adsorption in mesoporous matof capillary condensation / evaporation, but these types of isotherms can be reversible too (indicated by adsorption and desorption branches that lie on top of each other).

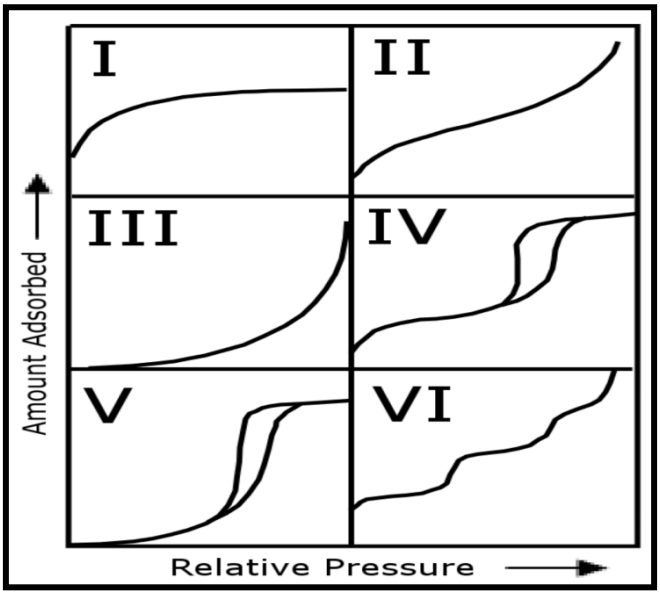

Fig.1.7 IUPAC classifications of gas adsorption isotherms

1.5.3 Diffuse reflection spectroscopy

Diffuse reflection spectroscopy is a type of spectroscopy where the diffuse reflection of radiation in the range ultraviolet to visible (190-800 nm) by a sample is measured. It helps in measuring band gap of semiconductor. In this dissertation, UV-Visible DRS was carried out using Hitachi H-3500 UV-Visible spectrophotometer (fig.1.8).

Fig. 1.8 UV-Visible spectrophotometer

1.5.4 Transmission electron microscopy (TEM)

Transmission electron microscopy is a quantitative microscopy technique in which a beam of electrons is transmitted through a sample to form an image. It sketches the transmission of a focused beam of electrons through a specimen, which in turn forms an image (fig 1.9).

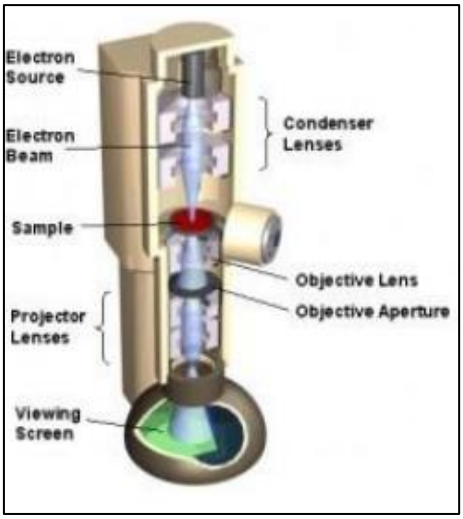

Fig 1.9 Transmission electron microscope

CHAPTER-2

LITERATURE REVIEW

Currently, semiconductor photo-catalysts driven by visible-light are the research focus techniques used to decompose organic compounds/pollutants. Since the major components of our solar energy are visible light (~44%) therefore, photo-degradation efficiency of organic compounds by photo-catalyst in visible light driven semiconductor photo-catalyst is expected to be better compared to UV-light-driven semiconductor photo-catalysts technique. However, photo-catalysts in the form of powder cause extra steps and costs to remove this powder from the slurry to prevent secondary pollution.

In a recent research work, V_2O_5 nanoflakes were fabricated by growing radially on PET fibres. Due to radial growth on PET fibres, the nano-flakes were flexible and had high surface area of polymeric fibres, therefore the Rhodamine B (RhB) could be degraded under visible light irradiation. The kinetics followed by photo-degradation of RhB solution was found to be 1st order with a constant rate of 0.0065 min^{-1}. This research work was successful. This indicated that V2O5 nano-flakes that were grown radially on PET fibre could possibly be used as organic waste water purifier under continuous flow condition [17].

Soylu *et al.*, 2016 prepared binary oxide catalysts by solid-state dispersion with various weight percentage of V_2O_5 loadings and the nano-composites were modified with surfactants. The binary oxide catalysts were used to degrade 2,4-dichlorophenol under ultraviolet irradiation to evaluate the photo-catalytic of the catalyst. The photocatalytic activities of the catalysts were evaluated in the degradation of 2,4-dichlorophenol under ultraviolet irradiation. The activity of 50 wt% V_2O_5-TiO_2 ($50V_2O_5$-TiO_2) was found to be higher than those of pure TiO_2, V_2O_5 and P25. The photo-catalytic efficiencies of the catalysts was affected by interactions between V_2O_5 and TiO_2. The efficiency of the $50V_2O_5$-TiO_2 catalyst was enhanced significantly by presence of cetyl trimethyl ammonium bromide (CTAB) and hexadecyl trimethyl ammonium bromide (HTAB). 100% degradation and highest reaction rate (2.22 mg/(L·min)) were obtained in 30 min with the catalyst. It was concluded that addition of a surfactant to the catalyst significantly enhanced the photo-catalytic activity by modifying the optical and electronic properties of TiO_2 and V_2O_5 [18].

Z. Karim *et al.*, 2015 prepared 20–40 nm vanadium(V) oxide nanoparticles by employing reverse micelles method using SDS as surfactant, ethanol and ethyl acetate as additives, hexane as continuous phase and water as disperse phase. V2O5 was formed under acid hydrolysis via ammonium metavanadate. The so synthesised nanoparticles were characterized by ultraviolet-visible(UV) spectroscopy, infrared(IR) spectroscopy, atomic force microscopy, and matrix-assisted laser desorption ionization (MALDI) mass spectrometry [19].

Tarasankar Pal *et al.*, 2014 synthesised ultra-long nanowires mediated by the intercalative properties of vanadium pentoxide (V_2O_5) using a pyridine–nitric acid (Py–HNO_3) system. It was noted that the introduction of HNO_3 in the reaction mixture as an additive with pyridine generated vanadium oxide with only +V oxidation state, which was ascertained from XPS analysis, whereas pyridine itself produced vanadium oxide with mixed valences. This energy efficient, time and cost effective proposition has been proved effective for the production of an industrially important oxidant without use of any surfactant or template. The as-produced V_2O_5 lead to the efficient degradation of dyes without using any extra oxidising agent. It was shown that degradation of the dyes complied electrostatically allowed 'adsorption–oxidation–desorption' mechanism [19].

Wen Chen *et al.*, 2013 modified TiO_2 nanotube arrays with V_2O_5 nanoparticles the electrophoresis deposition method. Catalyst showed significant enhancement on sunlight photo-degradation of crystal violet because of the role of interface and electronic transitions between V_2O_5 and TiO_2 [20].

Nilofar Asim *et al.*, 2008 synthesised V_2O_5 nanorod and nanoparticles using a surfactant-mediated method (based on CTAB). By applying different precursors and by varying reaction conditions within the CTAB soft template, morphologies of V_2O_5 nanostructures could be controlled. Nano-particles were synthesized in the size range of 45–160 nm by using sulphuric acid and ammonium metavandate as precursors. When vanadyl sulfate hydrate and sodium hydroxide were used as precursors nano-rods with lengths of 260–600 nm and diameters of 30–90 nm were yielded. Characterization was done by XRD, TEM, VPSEM and XPS. It was concluded that V_2O_5 nanoparticles and nanorods achieved better catalytic performance compared to bulk V_2O_5, i.e. workability at lower temperatures, lower onset temperature and higher H2 consumption (mol/g) [16].

RhB solution was degraded under UV and visible light irradiation using a mixture of ZnO (3.23 eV) and V_2O_5 (2.38 eV) nano-particles, respectively. The rod-like ZnO nanoparticles

had an average diameter of 244.1 ± 94.5 nm whereas sphere-like V_2O_5 nanoparticles had an average diameter of 231.9 ±14.0 nm. Under UV light irradiation, pure ZnO nanoparticles showed the highest photo-degradation efficiency having a rate constant of 0.034 ± 0.004 min^{-1}. This was due to high reducing power of its electrons and oxidation power of holes to produce free radicals. Whereas, pure V_2O_5 nano-particles demonstrated the highest photo-degradation efficiency under visible light irradiation having a rate constant of 0.013± 0.001 min^{-1} due to its profusion absorption in visible light region. The results of this research provided a useful guideline for designing a sunlight driven waste water purifier for organic pollutants removal based on a mixture of 2 semiconductor nano-materials, one having a wide bandgap and other having a narrow bandgap [21].

In this research work a binary oxide semiconductor photo-catalyst has been synthesised using clay as a support for adsorption. Photo-catalytic activity has been monitored by degrading methylene blue dye under UV as well as visible light. 100% degradation was observed in both the cases (UV and visible) using 1:1 clay-TiO_2-V_2O_5 nano-composites.

CHAPTER-3

METHODOLOGY

3.1 Materials

3.1.1 Reagents and chemicals used

Ammonium metavendate (99%), titanium butoxide, P25, ethanol (purity 99%), hydrochloric acid, methylene blue and bentonite were purchased from Loba chemie and used without further purification. Deionised and double distilled water was used for preparation of methylene blue solution and catalyst.

3.1.2 Instruments used

I. Weighing balance

Accurate quantities of used chemicals were measured with the help of weighing balance (SARTORIUS) Maximum-250 gm; Denisty-0.01 mg.

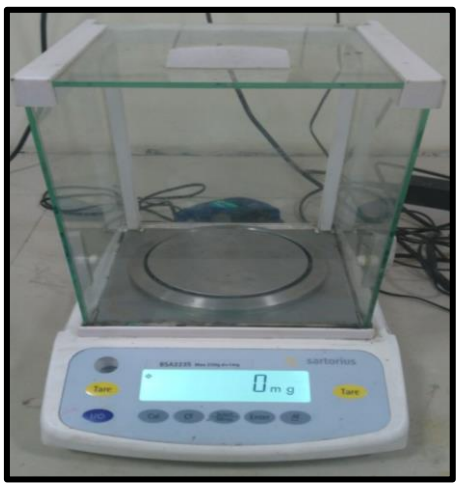

Fig. 2.1 Weighing balance

II. Magnetic Stirrer

A magnetic stirrer is a laboratory device which uses magnetic field to mix liquid samples, since only a small magnetic bar has to be put inside the sample to start the process of stirring. A REMI 2MLH is used in the experiment for mixing the three solutions, viz. clay, ammonium metavandate and titanium butoxide solution. Magnetic stirrer includes a hot plate or some other means for heating the liquid.

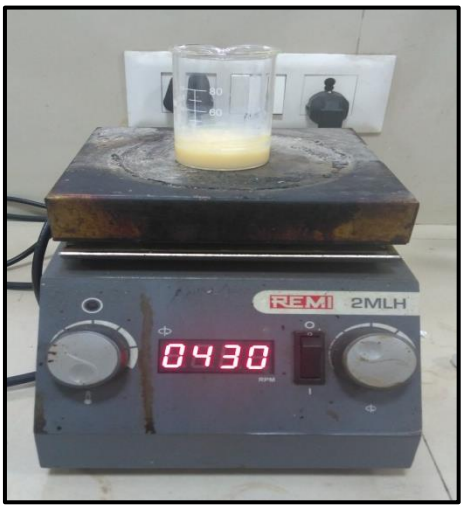

Fig.2.2 Magnetic stirrer

II. UV-Visible photo-reactor

This instrument includes a UV reactor (fig.3.3 (a)) and a visible reactor (fig. 3.3 (b)) . This is used to irradiate sample so that excitation of electrons takes place which results in generation of electron/hole pairs.

Fig. 2.3 UV-Visible photo-reactor

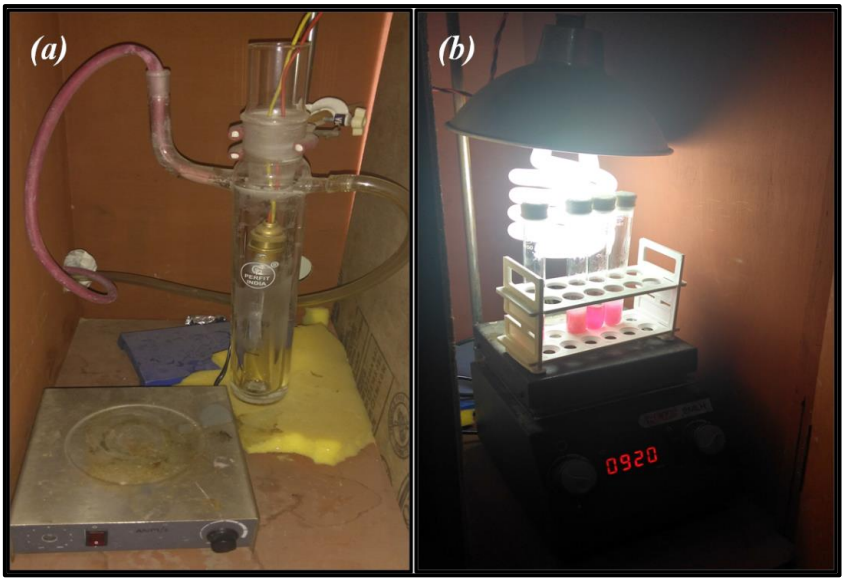

Fig. 2.4 (a) UV photo-reactor and **(b)** Visible photo-reactor.

IV. Microwave synthesis reactor

In a microwave synthesizer, microwave radiation is applied to produce chemical reactions. Microwaves act as high frequency electric field. It can heat any material that contains mobile electric charges. Polar solvents are heated as their component molecules are forced to rotate with the field and lose energy in collisions. In this dissertation an Ashton Paar (Microwave 300) has been used for the synthesis of nano-composites.

Fig. 2.5 Ashton Paar microwave synthesis reactor

V. Centrifuge machine

It is an equipment that puts an object in rotation around a fixed axis. It applies a strong potential force perpendicular to the axis of spin. After centrifugation, objects that are less dense are displaced and move to the center. In this dissertation, the microwaved reaction mixture was centrifuges at 8000rpm using a microprocessor based laboratory centrifuge (Fig. 3.5).

Fig. 3.5 Laboratory centrifuge

VI. UV-Visible spectrophotometer

UV-Vis spectroscopy is used in analytical chemistry for the quantitative determination of different analytes. Commonly, the spectroscopic analysis is carried out in solutions but it may also be studied in case of solids and gases. In this dissertation, UV-Visible spectrometer has been employed to study the degradation of methylene blue. Dye degradation is monitored by the decrease in absorption peak of dye (at 669 nm in case of methylene blue). Champion UV-Visible spectrometer has been used (fig.3.7).

Fig. 3.7 UV-Visible spectrophotometer

VII. Hot Air Oven

The hot air oven also known as digital temperature indicator cum controller of PHYSILAB was used to dry the prepared nano-composites. The product was dried overnight at 60˚C.

Fig. 3.8 Hot air oven

3.2 Methods

3.2.1 Synthesis of clay-TiO_2-V_2O_5

200mg of clay was taken in 20mL water and kept on stirring for 2hours. Two solutions, each of ammonium metavandate and titanium butoxide respectively were prepared as follows:

I. Solution of ammonium metavandate was prepared by adding 96.5gm ammonium metavandate in 5mL water + 5mL ethanol and kept on stirring at 70° C for one hour to obtain a yellow solution.

II. Solution of titanium butoxide was prepared by adding 2mL titanium butoxide in 5mL water. 4mL HCl was added afterwards to remove turbidity.

Solution I was added slowly in the clay slurry followed by addition of solution II and stirred for 2 hours after which the reaction mixture was kept in microwave at 150° C for 30minutes. The final product so obtained was centrifuged at 8000 rpm for 1 minute and washed with water 4-5 times and dried overnight at 60° C. The dried product was collected and used further for characterisation and application in dye degradation.

Following the same procedure two other catalysts were prepared by varying the concentration of ammonium metavandate and keeping the concentration of clay-titanium butoxide unchanged.

Methodology

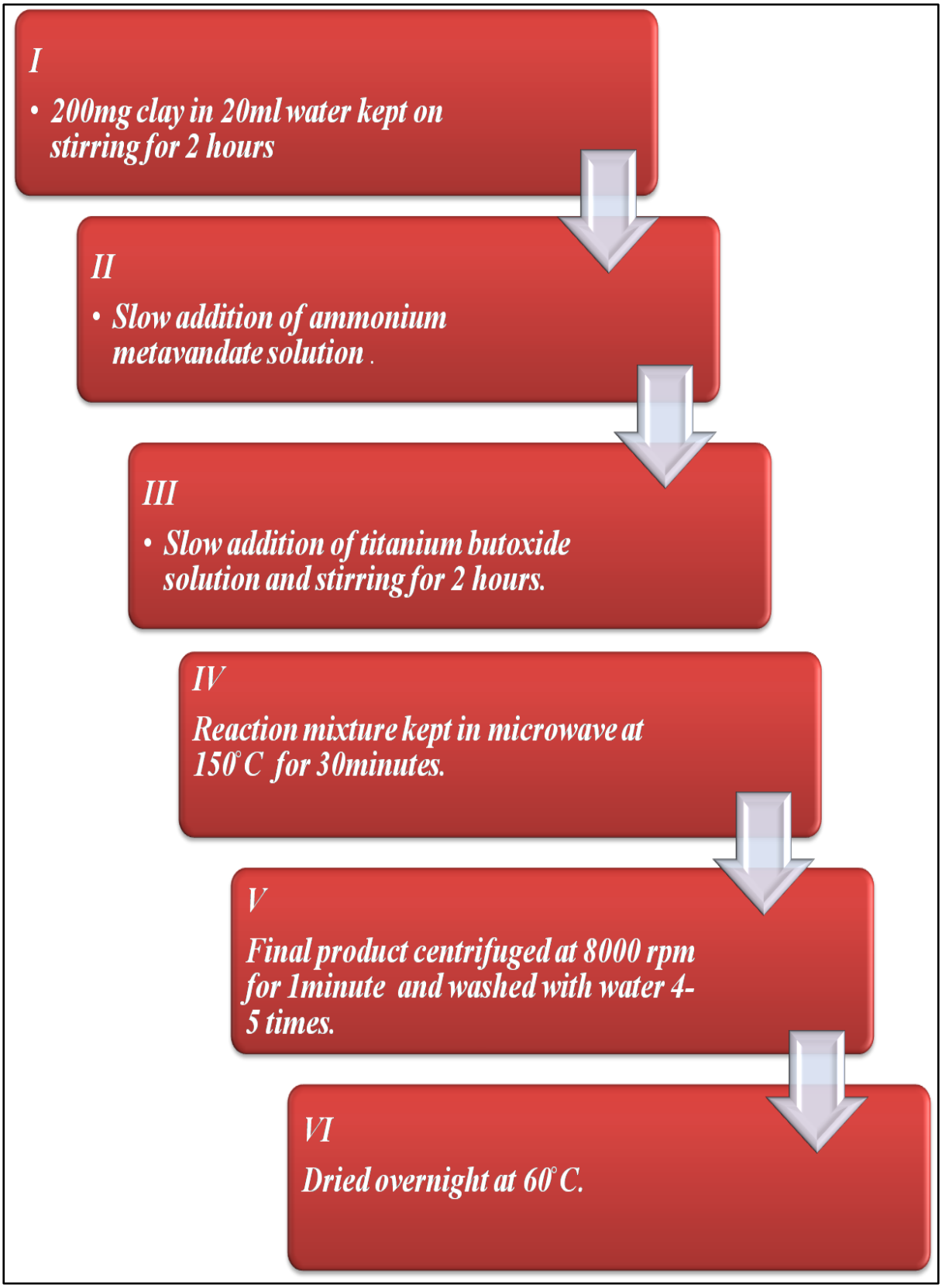

3.2.2 Synthesis of Clay TiO_2

Clay TiO_2 was synthesised by a similar process mentioned above. Solution of only titanium butoxide was prepared by adding 2 mL titanium butoxide in 5 mL water. 4 mL HCl was added afterwards to remove turbidity. It was added slowly in the clay solution and stirred for 2 hours after which the reaction mixture was kept in microwave at 150° C for 30minutes. The final product so obtained was centrifuged at 8000 rpm for 1 minute and washed with water 4-5 times and dried overnight at 60° C.

3.2.3 Typical procedure for dye degradation

The dye degradation was carried out with as-synthesised clay-TiO_2-V_2O_5 composites in which clay-TiO_2 and V_2O_5 were in the ratio- 1:1, 1:2 and 1:3 with a catalytic dose of 0.25g per litre in 20 mL (10^{-4} M concentration) of dye. Clay-TiO_2 and P25 were also taken for comparison. The photocatalytic activity was carried out by using 65 Watt Compact Fluorescent Light (CFL) lamp as a visible light source and 100 Watt mercury lamp as UV light source. Before illumination, the dye solution containing catalyst was stirred in dark for 30 minutes to establish adsorption-desorption equilibrium. The dye solution containing the catalyst was irradiated for 10, 20, 30, 60 and 90 minutes. The distance between the solution and the lamp was kept 10 cm. After each photocatalytic process the dye was separated from catalyst by centrifugation and subsequently filtered using 0.22μm syringe filters. The spectra of residual dye was taken using UV-Visible spectrophotometer (Analytik jena ***SPECORD*** 205). Absorbance spectra of residual dye samples were recorded corresponding to absorption peak at 669 nm. According to beer-lambert's law ($A= \varepsilon Cl$, where C is the concentration and A is the absorbance), since absorbance is directly proportional to concentration of dye, therefore, the degradation efficiency can be found as R where C_0, C, A_0 and A represent concentration and absorbance of dye at time 0 and t respectively.

CHAPTER-4

RESULTS AND DISCUSSIONS

4.1 Characterization

4.1.1 Diffuse reflectance spectroscopy (DRS)

Excitation edge of clay-TiO_2 is red-shifted upon incorporating V_2O_5 as shown in figure 4.1. The red-shift clearly indicates the improvement in visible light absorption of clay-TiO_2 by incorporation of V_2O_5. This also leads to the decrease in band gap energy of the nano-composite (Fig.4.1) making it applicable under visible light.

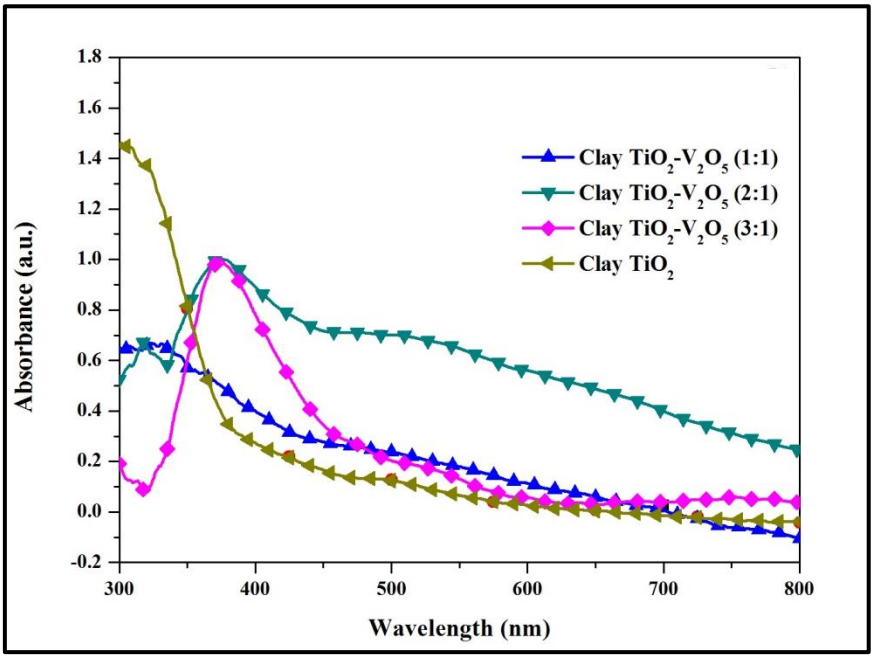

Fig. 4.1 DRS pattern of catalysts employed

4.1.2 X-ray diffraction pattern:

From X-ray diffraction pattern (Fig. 4.2(b)) of V_2O_5-TiO_2/clay nano-composites, peaks of anatase TiO_2 were found which exist at 2θ = 25.62, 36.06, 48.71 and 54.99 degree corresponding to (101), (200) and (105) (JCPDS file Number:75-1537) diffraction planes respectively. Peaks of V_2O_5 (Fig 4.2 (b)) (JCPDS file Number: 78-1510) were found to be absent from our as-synthesized V_2O_5/Clay-TiO2 nanocomposites (0.2- 0.6%). The V_2O_5

peaks are absent due to their low content which may be below the detection limit. Only a single peak for V_2O_5 in 0.4% V_2O_5-TiO_2/clay nano-composite was found at 2θ= 38.11 degree corresponding to (111) (JCPDS file Number: 04-0783) diffraction plane of V_2O_5 which may be due to low V_2O_5 content [22, 23]. This peak diminishes at the much lower content in case of 0.2% V_2O_5-TiO_2/clay due to their low content of V_2O_5 which may be below the detection limit (Fig. S_4, supporting information). The peak at 2θ= 7.74 (fig. 4.2(c)) in clay (JCPDS file Number: 03-0019) corresponds to *d*(001) basal spacing of its layered structure [15]. The other peaks present at 2θ=18.61, 19.80, 26.55, 28.40, 35.30 and 54.23 are due to some excess silica (JCPDS file Number: 84-0384) in clay. The standard XRD data of TiO_2, V_2O_5 NPs and clay are shown in Fig. 4.1 to compare the diffraction peaks.

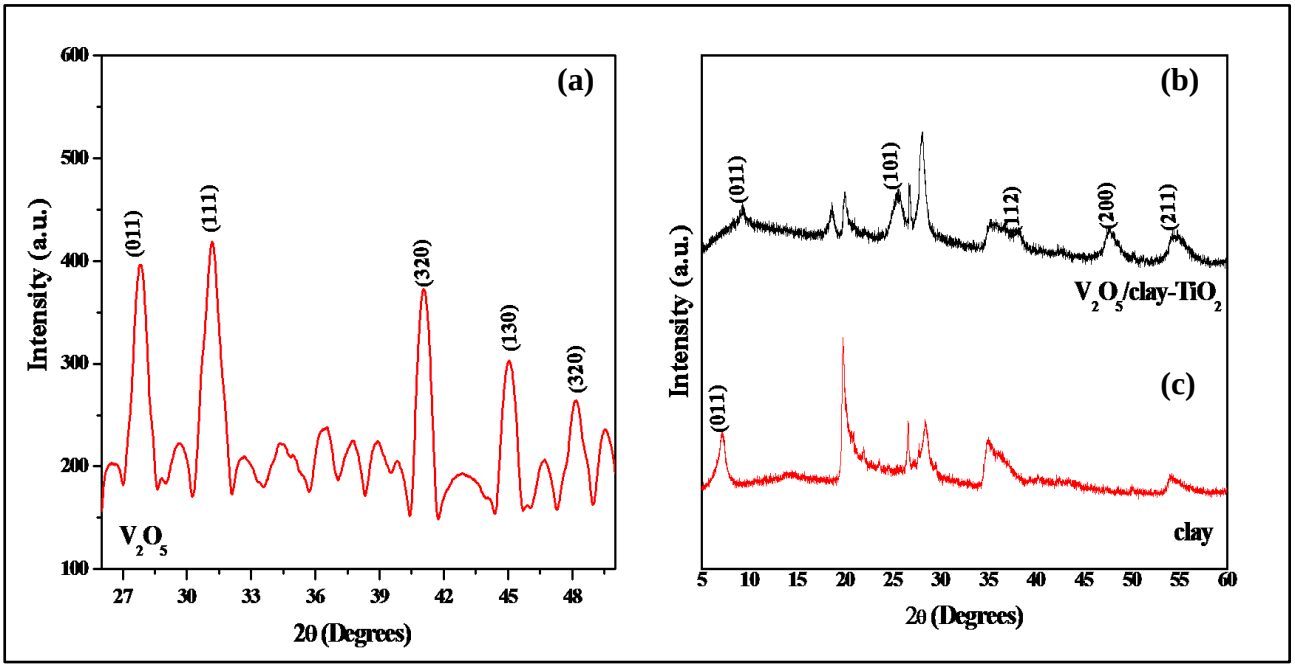

Fig. 4.2 XRD pattern of **(a)** V_2O_5 nanoparticles; **(b)** V_2O_5/clay-TiO_2 and **(c)** clay.

4.1.3 BET analysis

From N_2 adsorption-desorption measurements (Fig. 4.3) surface area of the Clay- TiO_2 nano-composites was found to be maximum at 94 m^2/g with pore volume 0.3302 cm^3/g. Upon V_2O_5 loading (0.2-0.6 % loading) both surface area and pore volume decreased to 77 m^2/g and 0.3175cm^3/g respectively. This decrease in surface area and pore volume may have occurred due to the filling of vacant pores of the TiO_2/clay nano-composite by V_2O_5 nano-particles. But, the pore size distribution is not affected much by V_2O_5 loading.

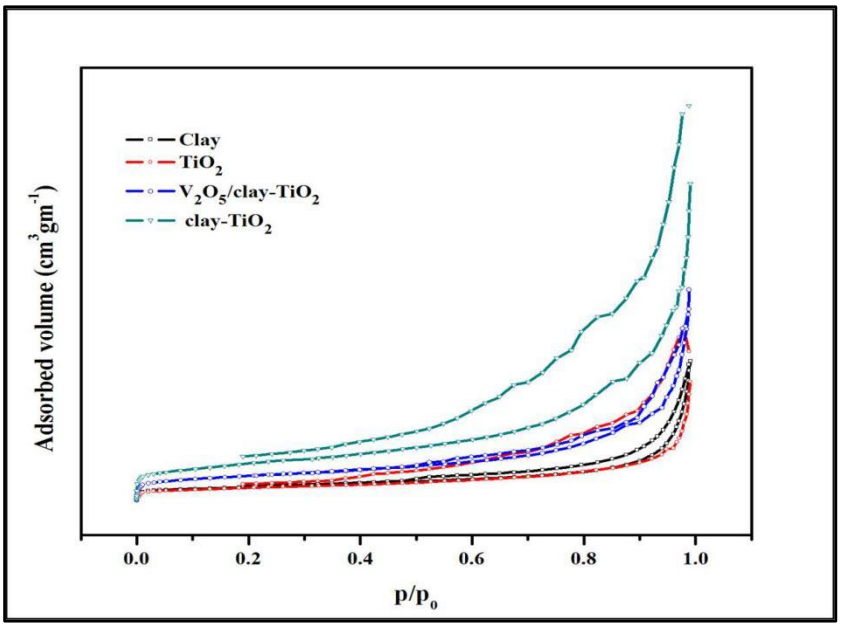

Fig. 4.3 BET analysis of different catalyst

Conditions for BET sample have been listed in table. 4.1.

Table 4.1- Conditions for BET samples

Ambient Temp	N_2 % in Cylinder	Regeneration Temperature	Regeneration Time	Sample Dry Wt.	Injected N_2 vol.	Sample Loss (%)
25^0C	70%	150^0C	3 hours	23.39g	5cc	0.00%

The values of the specific surface area and pore volume of all the nanocomposites have been listed in Table 4.2.

Table 4.2 Textural characteristics for different catalysts determined from nitrogen sorption measurements.

Catalyst	Surface Area (m^2g^{-1})	Pore Volume (cm^3g^{-1})
Clay-TiO_2	94	0.3302
V_2O_5/Clay-TiO_2	77	0.3175
TiO_2	71	0.2236
Clay	65	0.2001

4.1.4 Transmission electron microscopy

Following images of nanocomposites were observed through transmission electron microscope.

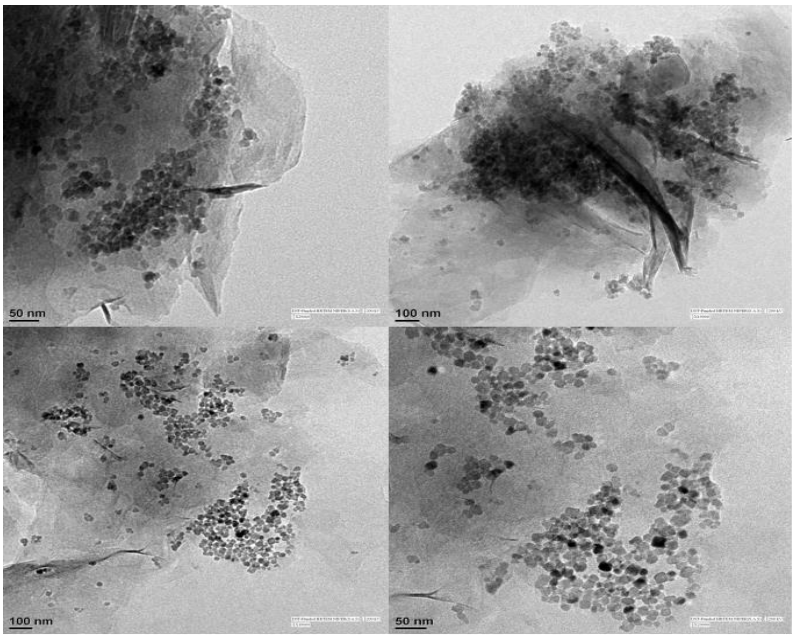

Fig 4.4 TEM images of Clay-TiO_2/V_2O_5 nano-composite

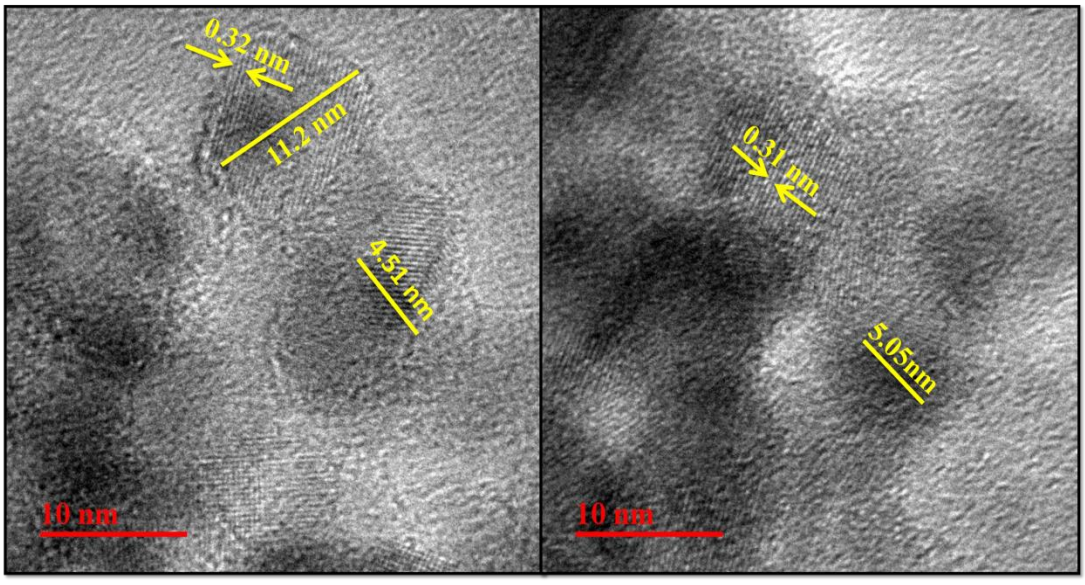

Fig 4.5 Enlarged TEM images of Clay-TiO_2/V_2O_5 nano-composite showing d-spacing.

From TEM images it can be observed that TiO_2 and V_2O_5 nano particles have been successfully impregnated upon clay. V_2O_5 nanoparticles are found to be deposited upon tiO2

nanoparticles as observed from high magnification images which can facilitate better electron transfer from V_2O_5 to TiO_2.

The particle size of TiO_2 nanoparticles as observed from hrtem images are found to be 11.2nm having average d-spacing of 0.31nm and those of V_2O_5 were 4.51nm.

4.2 Adsorption and Photocatalytic activity

4.2.1 Adsorption and photo-catalytic activity of 1:1 Clay-TiO_2/V_2O_5 nano-composite

Clay-TiO_2 nano-composite having 0.2% V_2O_5 loading showed 100% degradation under both UV and visible irradiation with 0.25g/litre catalyst in 20mL dye. The dye degraded completely in 90minutes owing to the presence of TiO_2 under UV irradiation (fig. 4.4(b)) and V_2O_5 under visible light irradiation(fig. 4.4(c)).

The adsorption in dark can be attributed to the presence of clay. (fig.4.4 (a))

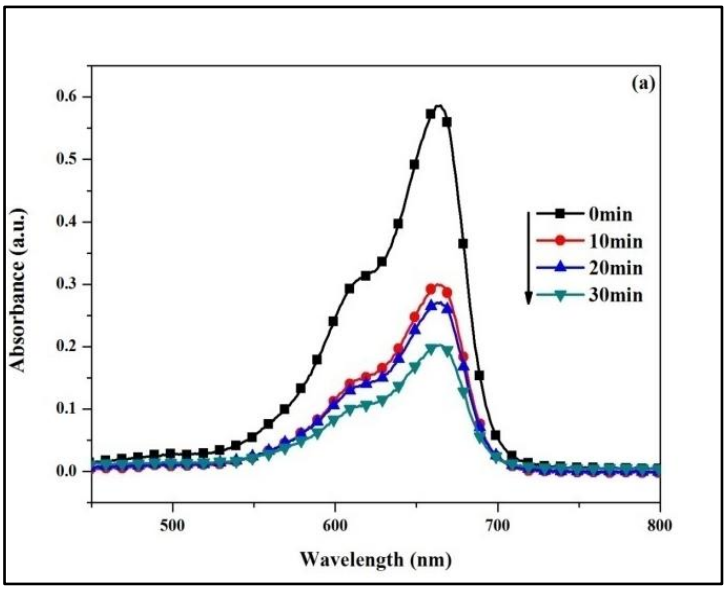

Fig. 4.6 (a) Adsorption in dark (1:1 Clay-TiO_2/V_2O_5)

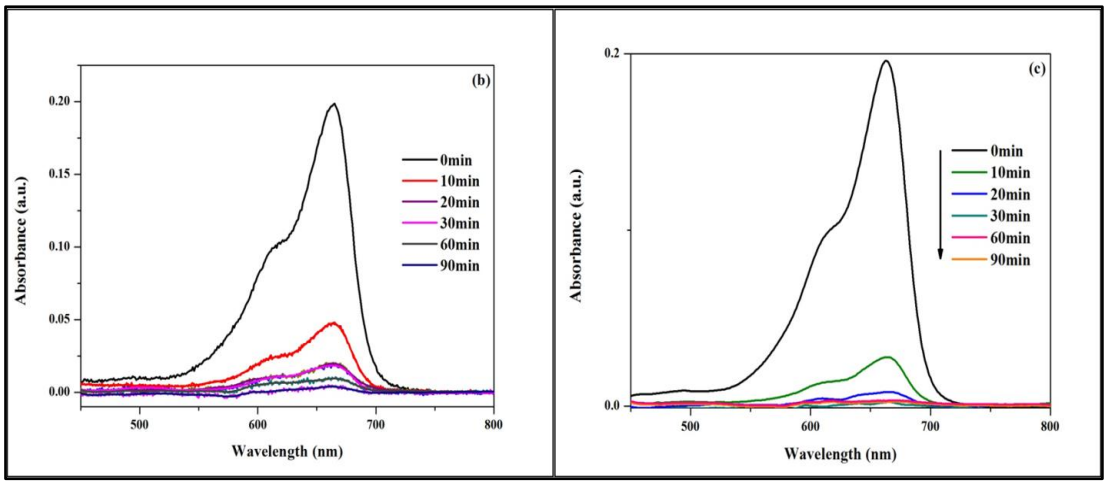

Fig.4.6 Degradation shown by 1:1 Clay-TiO_2/V_2O_5 under **(b)** UV irradiation and **(c)** visible irradiation

4.2.2 Adsorption and photo-catalytic activity of 1:2 Clay-TiO_2/V_2O_5 nano-composite

Nano-composite having 0.4% V_2O_5 showed 100% degradation under visible irradiation (fig. 4.5 (c)) but could not degrade the dye completely under UV irradiation (fig. 4.5 (b)) in 90 minutes. This can be due to the reason that increasing the amount of V_2O_5 causes a decrease in the activity of TiO_2 which is active under UV irradiation. This can be then concluded that any further increase in the amount of V_2O_5 would cause a decrease in its activity under UV irradiation. This was proved to be true as a further increase in amount of V_2O_5 caused further decrease in catalyst's activity under UV light (section 4.2.3)

There was not much change recorded in the adsorption by the catalyst in dark.(fig. 4.5 (a))

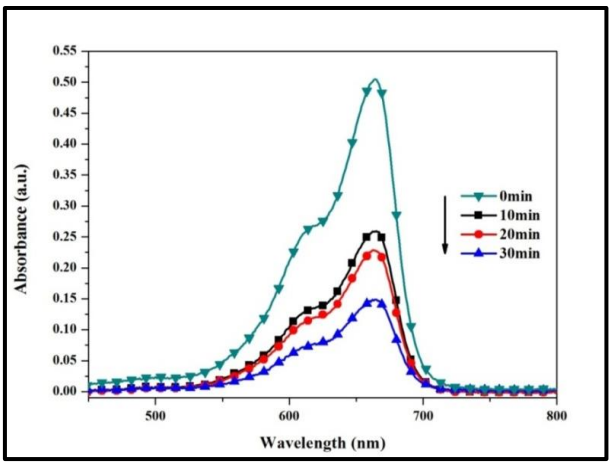

Fig. 4.7 (a) Adsorption in dark (1:2 Clay-TiO_2/V_2O_5)

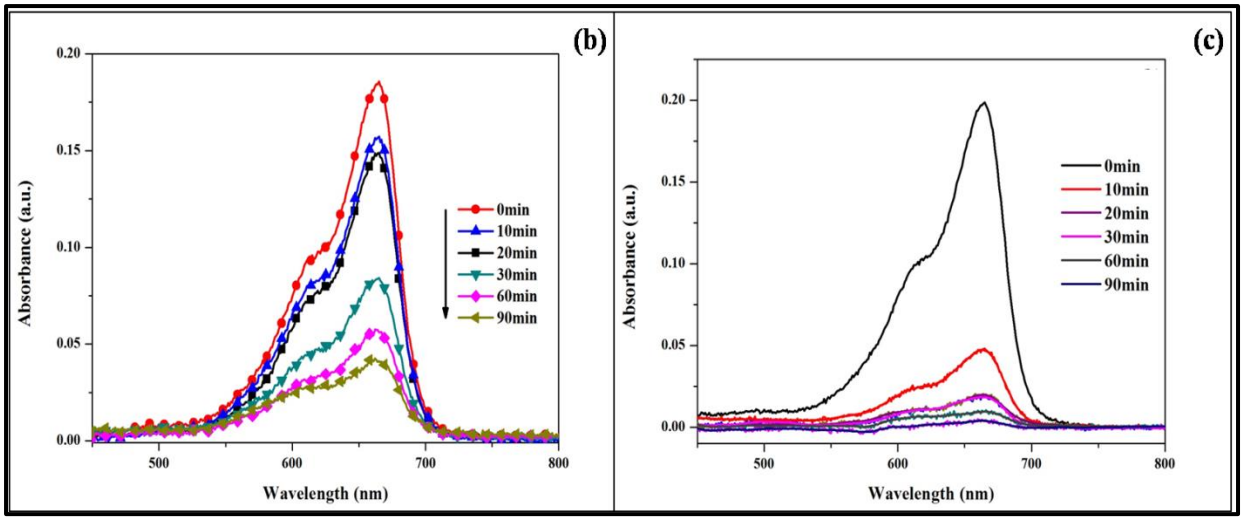

Fig.4.7 Degradation shown by 1:2 Clay-TiO_2/V_2O_5 under **(b)** UV irradiation and **(c)** visible irradiation

4.2.3 Adsorption and photo-catalytic activity of 1:3 Clay-TiO_2/V_2O_5 nano-composite

Nano-composite having 0.6% V_2O_5 concentration showed 100% degradation under visible irradiation (fig. 4.6 (c)) but could not degrade the dye completely under UV irradiation (fig. 4.6 (b)) in 90 minutes. The reason has already been discussed in section 4.2.2.

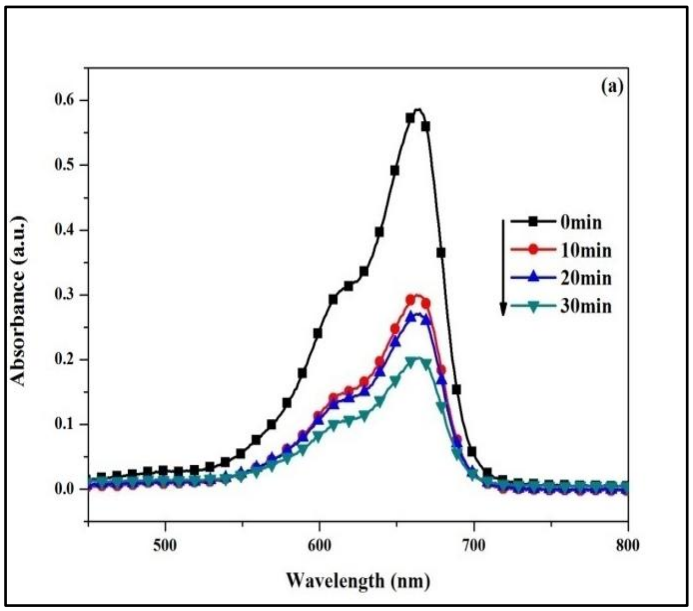

Fig. 4.8 (a) Adsorption in dark (1:3 Clay-TiO_2/V_2O_5)

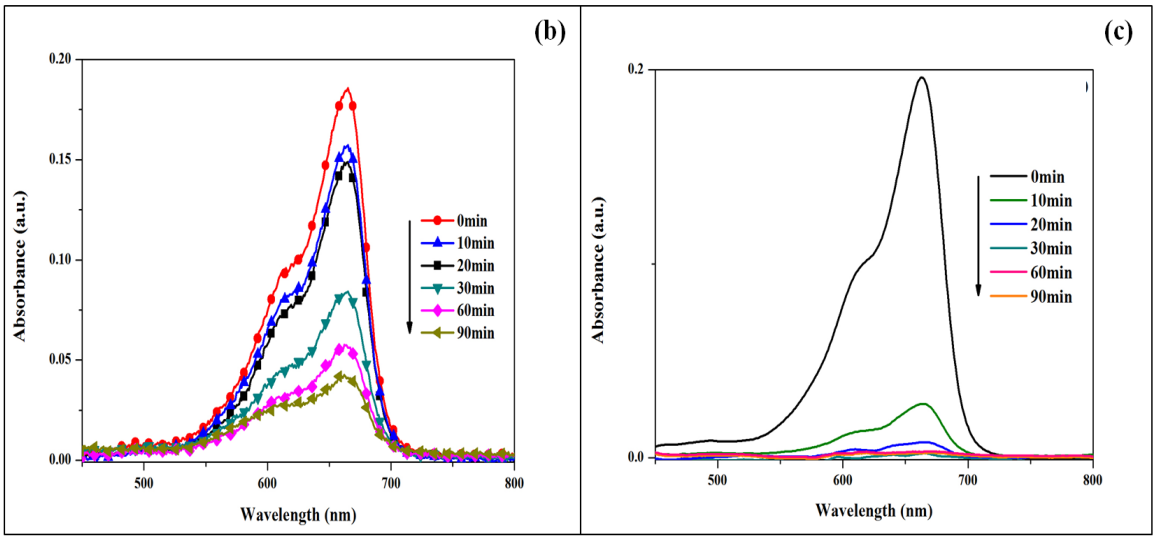

Fig.4.8 Degradation shown by 1:3 Clay-TiO_2/V_2O_5 under **(b)** UV irradiation and **(c)** visible irradiation

4.2.4 Adsorption and photo-catalytic activity of Clay TiO_2

Nano-composite having only Clay-TiO_2 showed 60% degradation under UV irradiation in 90 minutes but could not degrade dye as efficiently under visible irradiation. This can be attributed to the fact that TiO_2 has a large band gap (~3.2 eV) that can only be excited under UV irradiation.

The adsorption in dark was nearly the same as above 3 cases.

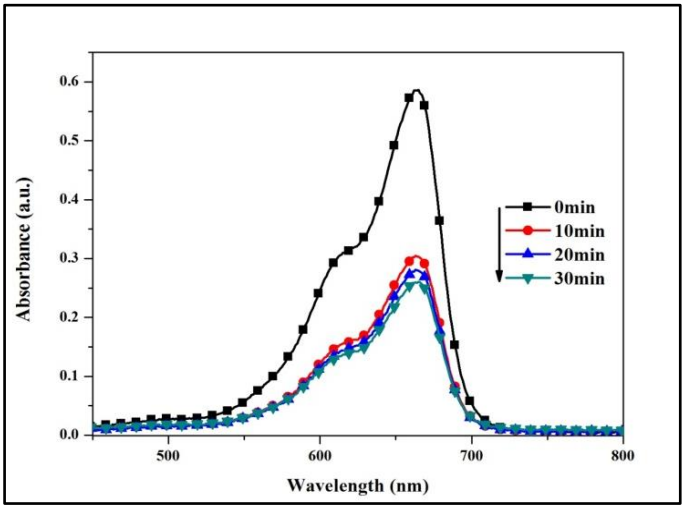

Fig. 4.9 (a) Adsorption in dark (Clay-TiO_2)

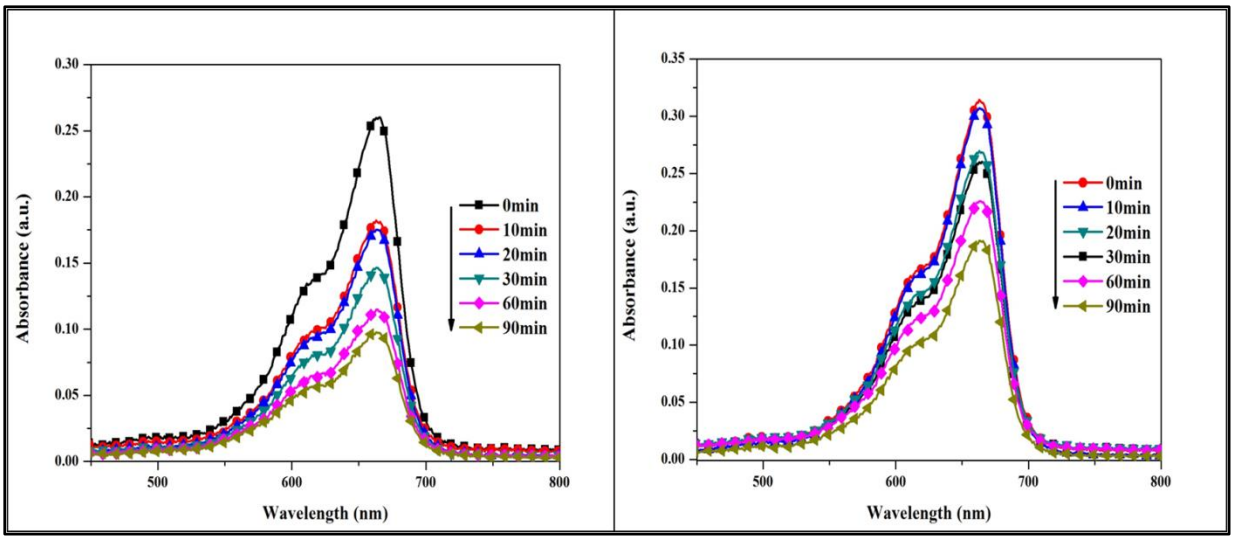

Fig.4.9 Degradation show by Clay-TiO_2 under **(b)** UV irradiation and **(c)** visible irradiation

4.2.5 Adsorption and photo-catalytic activity of P25

Commercially available P25 showed 40% degradation under UV light irradiation, but showed only 10% degradation under visible light.

Adsorption in dark was negligible as compared to other 4 cases because of absence of clay content.

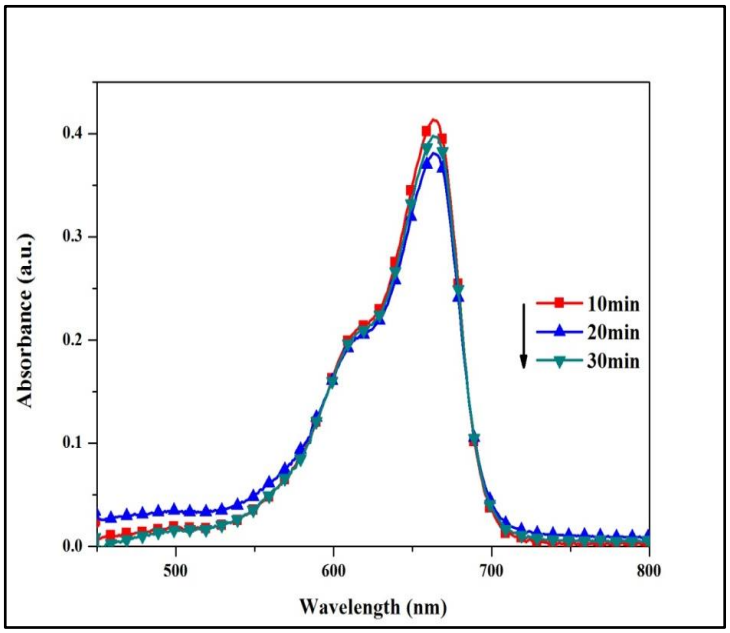

Fig. 4.10 (a) Adsorption in dark (P25)

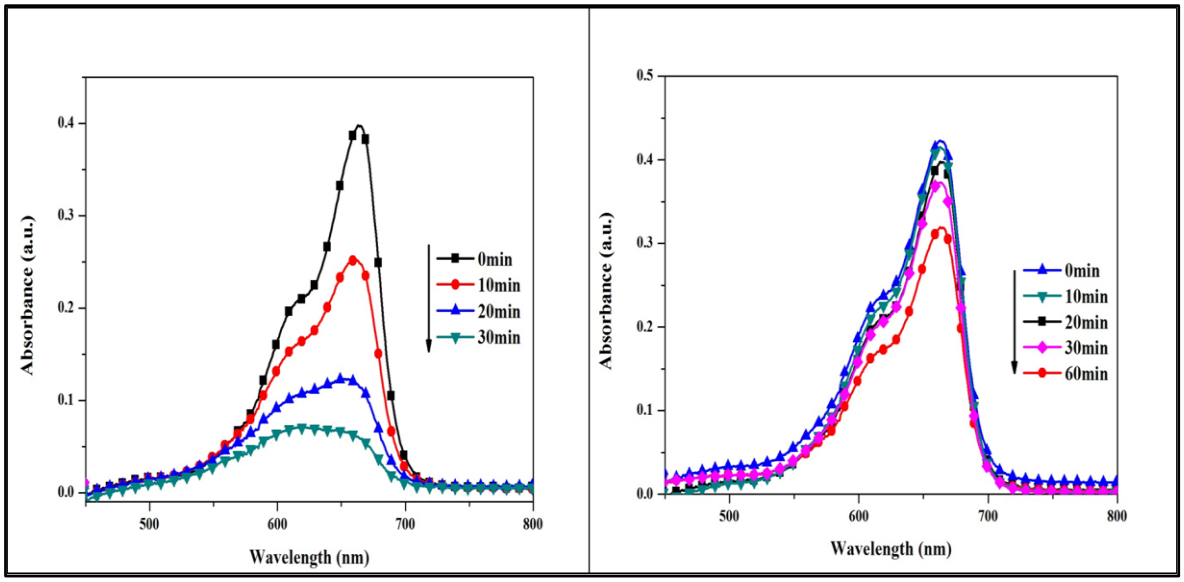

Fig.4.10 Degradation show by P25 under **(b)** UV irradiation and **(c)** visible irradiation

4.3 Overlay of photo-catalytic activity

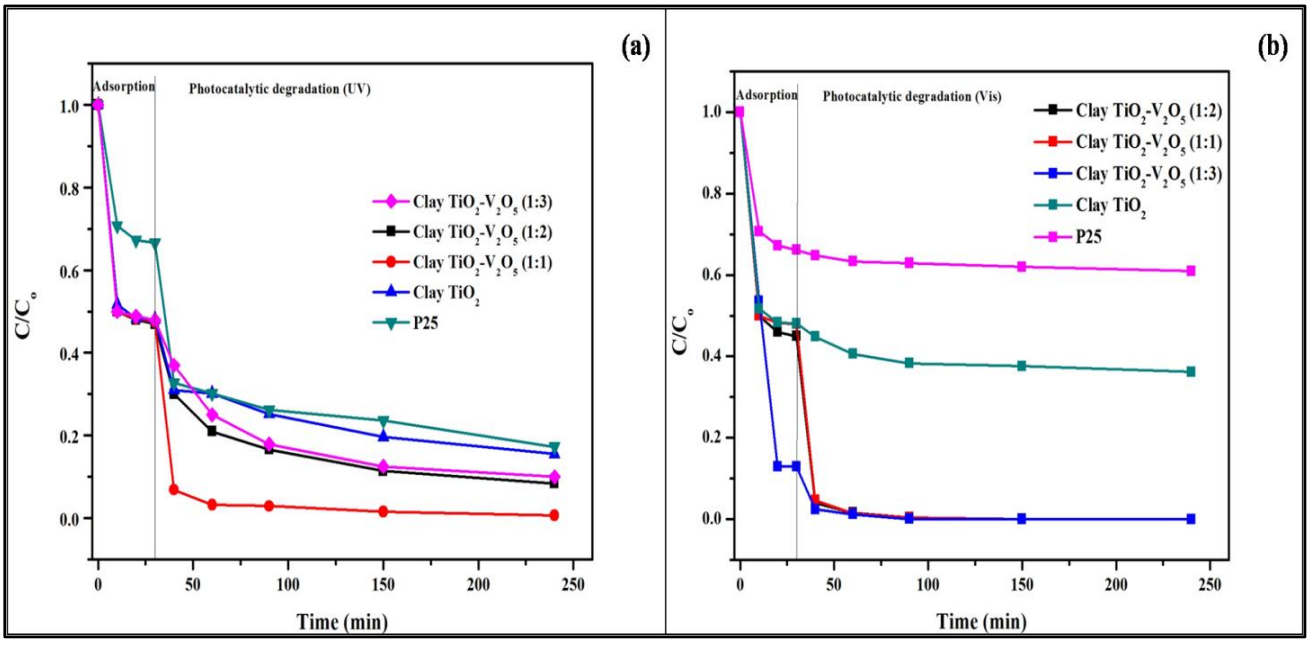

Fig. 4.11 Overlay of photocatalytic activity under **(a)** UV irradiation and **(b)** visible irradiation

4.3.1 UV irradiation

Under UV irradiation, clay TiO_2 composite having 0.2% V_2O_5 (1:1) was found to exhibit the best photocatalytic activity (100% degradation) amongst the 5 catalysts employed in dye degradation. This is because incorporation of V_2O_5 leads to the decrease in band gap energy of the nano-composite that helps in efficient generation of electron-hole pairs. Further increase of V_2O_5 leads to decrease in degradation under UV irradiation. This might be possible because further increase of V_2O_5 starts to hinder the activity of TiO_2 as V_2O_5 itself is only active under visible irradiation.

P25 shows the least degradation followed by clay-TiO_2 being the second best.

Catalyst	*%Degradation*
Clay-TiO_2-V_2O_5 (0.2%)	100%
Clay-TiO_2-V_2O_5 (0.4%)	90%
Clay-TiO_2-V_2O_5 (0.6%)	87%
Clay-TiO_2	80%
P25	75%

Table 4.2 Photocatalytic activity under UV light irradiation

4.3.2 Visible irradiation

All catalysts containing V_2O_5 showed 100% degradation under visible light. This is due to short band gap of V_2O_5 which makes it active under visible irradiation. clay-TiO2 having large band gap showed 50% degradation, whereas commercially available P25 showed 25% degradation due to absence of clay.

Catalyst	*%Degradation*
Clay-TiO_2-V_2O_5 (0.2%)	100%
Clay-TiO_2-V_2O_5 (0.4%)	100%
Clay-TiO_2-V_2O_5 (0.6%)	100%
Clay-TiO_2	50%
P25	25%

Table 4.3 Photocatalytic activity under Visible light irradiation

4.4 Comparison of photo-catalytic activity

4.4.1 Under UV light irradiation

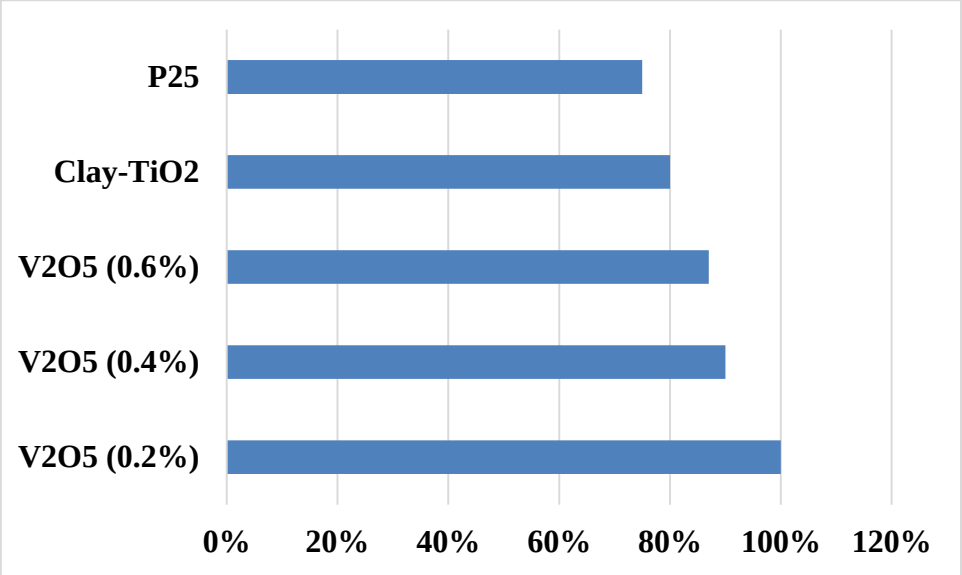

Fig 4.12 Comparison graph of photocatalytic activity of various catalysts under UV light irradiation

4.4. Under visible light irradiation

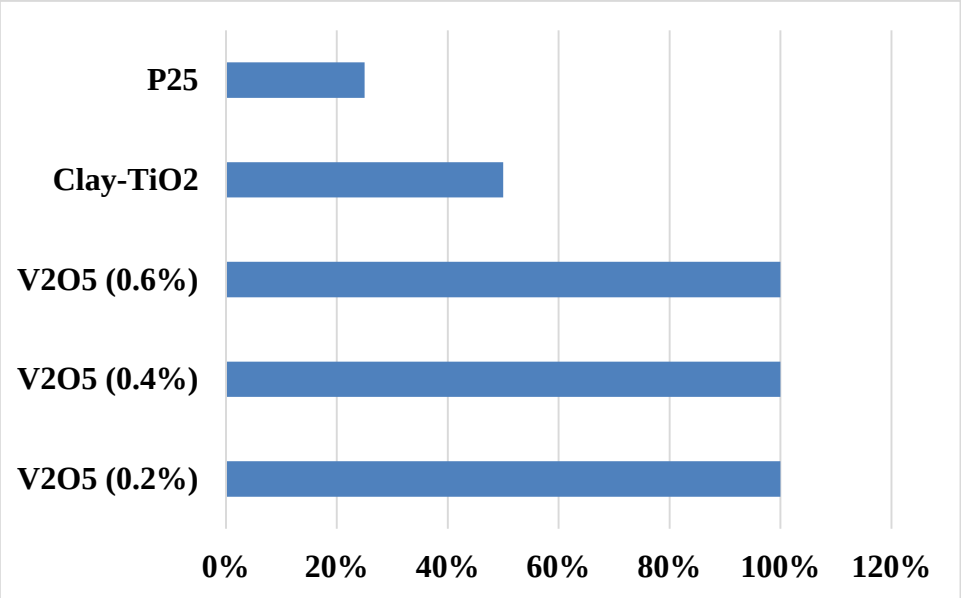

Fig 4.13 Comparison graph of photocatalytic activity of various catalysts under Visible light irradiation

CHAPTER-5

CONCLUSION

The TiO_2-clay/V_2O_5 nanocomposites were synthesized by simple microwave irradiation method. The synthesized nano-composites were found to be highly porous having uniform pore size distribution. The photocatalytic activity of TiO_2-clay/V_2O_5 nanocomposite was found to be higher than that of TiO_2-clay nanocomposites under UV irradiation wherein V_2O_5 acts as a sensitizer which enhances the activity of TiO_2-clay in visible region by decreasing the energy band gap. The TiO_2-clay/V_2O_5 nano-composites having 0.2% V_2O_5 content showed excellent photo-catalytic activity under both UV and visible irradiation. On increasing V_2O_5 content beyond 0.2% by weight, the photocatalytic activity reduced under UV light irradiation. This may be due to the reason that increasing the amount of V_2O_5 causes a decrease in the activity of TiO_2 which is active under UV irradiation. In this research, presence of clay plays a crucial role to provide a stable and hydrophobic nano-composite along with a porous network which makes it easy to separate and recycle. Therefore, TiO_2-clay/V_2O_5 nano-composites can prove to be efficient photo-catalyst for usage in decontamination of air and water resources which nowadays is one of the greatest challenges for mankind.

CHAPTER-6

REFERENCES

1. Rauf, M. and S.S. Ashraf, *Fundamental principles and application of heterogeneous photocatalytic degradation of dyes in solution.* Chemical engineering journal, 2009. **151**(1): p. 10-18.
2. Yang, X., et al., *Rapid degradation of methylene blue in a novel heterogeneous Fe3O4@ rGO@ TiO2-catalyzed photo-Fenton system.* Scientific reports, 2015. **5**.
3. Mehta, A., et al., *Effect of silica/titania ratio on enhanced photooxidation of industrial hazardous materials by microwave treated mesoporous SBA-15/TiO2 nanocomposites.* Journal of Nanoparticle Research, 2016. **18**(7): p. 209.
4. Lachheb, H., et al., *Photocatalytic degradation of various types of dyes (Alizarin S, Crocein Orange G, Methyl Red, Congo Red, Methylene Blue) in water by UV-irradiated titania.* Applied Catalysis B: Environmental, 2002. **39**(1): p. 75-90.
5. Houas, A., et al., *Photocatalytic degradation pathway of methylene blue in water.* Applied Catalysis B: Environmental, 2001. **31**(2): p. 145-157.
6. Marcı, G., et al., *Photocatalytic oxidation of toluene on irradiated TiO 2: comparison of degradation performance in humidified air, in water and in water containing a zwitterionic surfactant.* Journal of Photochemistry and Photobiology A: Chemistry, 2003. **160**(1): p. 105-114.
7. Dong, H., et al., *An overview on limitations of TiO 2-based particles for photocatalytic degradation of organic pollutants and the corresponding countermeasures.* Water research, 2015. **79**: p. 128-146.
8. Rhouta, B., et al., *Surfactant-modifications of Na+–beidellite for the preparation of TiO 2–Bd supported photocatalysts: II—Physico-chemical characterization and photocatalytic properties.* Applied Clay Science, 2015. **115**: p. 266-274.
9. Rhouta, B., et al., *Surfactant-modifications of Na+-beidellite for the preparation of TiO 2-Bd supported photocatalysts: I-organobeidellite precursor for nanocomposites.* Applied Clay Science, 2015. **115**: p. 260-265.

10. Chen, D., H. Zhu, and X. Wang, *A facile method to synthesize the photocatalytic TiO 2/montmorillonite nanocomposites with enhanced photoactivity.* Applied Surface Science, 2014. **319**: p. 158-166.
11. Chen, D., et al., *Synthesis and characterization of TiO 2 pillared montmorillonites: application for methylene blue degradation.* Journal of colloid and interface science, 2013. **409**: p. 151-157.
12. Liu, J., et al., *Solvothermal preparation of TiO 2/montmorillonite and photocatalytic activity.* Applied Clay Science, 2009. **43**(2): p. 156-159.
13. Yang, C., et al., *Hydrothermal synthesis of TiO 2–WO 3–bentonite composites: conventional versus ultrasonic pretreatments and their adsorption of methylene blue.* Applied Clay Science, 2015. **105**: p. 243-251.
14. Sun, S., et al., *Enhanced photocatalytic activity of microwave treated TiO 2 pillared montmorillonite.* Materials Chemistry and Physics, 2006. **98**(2): p. 377-381.
15. Mishra, A., et al., *Enhanced heterogeneous photodegradation of VOC and dye using microwave synthesized TiO 2/Clay nanocomposites: A comparison study of different type of clays.* Journal of Alloys and Compounds, 2017. **694**: p. 574-580.
16. Asim, N., et al., *Vanadium pentoxide: synthesis and characterization of nanorod and nanoparticle V 2 O 5 using CTAB micelle solution.* Microporous and Mesoporous Materials, 2009. **120**(3): p. 397-401.
17. Chan, Y.-L., S.-Y. Pung, and S. Sreekantan, *Synthesis of V2O5 Nanoflakes on PET Fiber as Visible-Light-Driven Photocatalysts for Degradation of RhB Dye.* Journal of Catalysts, 2014. **2014**.
18. Sinirtas, E., M. Isleyen, and G.S.P. Soylu, *Photocatalytic degradation of 2, 4-dichlorophenol with V 2 O 5-TiO 2 catalysts: Effect of catalyst support and surfactant additives.* Chinese Journal of Catalysis, 2016. **37**(4): p. 607-615.
19. Roy, A., et al., *Facile synthesis of pyridine intercalated ultra-long V 2 O 5 nanowire from commercial V 2 O 5: catalytic applications in selective dye degradation.* CrystEngComm, 2014. **16**(33): p. 7738-7744.
20. Zhao, C., et al. *V 2 O 5 Modified TiO 2 Nanotube Array Catalysts for Degradation of Crystal Violet Using Solar Energy*. in *Nanophotonics, Nanoelectronics and Nanosensor*. 2013. Optical Society of America.
21. Chan, Y.L., S.Y. Pung, and S. Sreekantan, *STUDY OF ZnO and V2O5 NANOPARTICLES AS HETEROGENEOUS PHOTOCATALYSTS IN DEGRADING ORGANIC POLLUTANTS.*

22. Nguyen, D.B., et al., *Preparation, characterization and evaluation of catalytic activity of titania modified with silver and bentonite.* Journal of Industrial and Engineering Chemistry, 2012. **18**(5): p. 1764-1767.
23. Liu, J., et al., *Preparation and photocatalytic activity of silver and TiO 2 nanoparticles/montmorillonite composites.* Applied Clay Science, 2007. **37**(3): p. 275-280.